Proceedings in Manufacturing Systems
Proceedings in Manufacturing Systems, Volume 17, Issue 4, 2022, 147-152 ISSN 2067-9238

CASE STUDY OF STRUCTURES BASED ON HYPERBOLIC GEOMETRY

Patricia Isabela BRAILEANU[1,*]

[1)] Lecturer PhD. Eng., Department of Machine Elements and Tribology, University "Politehnica" of Bucharest, Romania

Abstract: *Structures based on hyperbolic surfaces are present in various fields, both in industrial engineering as integral parts of a structural ensemble, as well as in domains such as architecture or even art. Most often, this type of structure can be found in industry within the cooling structures of oil refineries or petrochemical plants as cooling towers. This article aims to analyze a form built based on a hyperboloid of one sheet, to which structures intended to strengthen the overall geometry have been added as ribs. Multiple iterations of the same geometry have been generated, ranging from the basic geometry without ribs to the basic geometry with the addition of 10 ribs. The analysis can provide valuable insights into how these reinforcing elements can enhance the overall integrity and performance of the hyperboloid–based structures. The research aims to enhance understanding of the mechanical performance of these structures and their potential for use in practical applications.*

Key words: *hyperboloid structure, reinforced structures, static analysis.*

1. INTRODUCTION

A hyperboloid is a 3D surface generated by rotating a hyperbolic curve around an axis and it can take different forms depending on how the hyperbola rotates around its axis: hyperboloid of one sheet (Fig. 1,*a*), hyperboloid with a conical surface in between (Fig. 1,*b*), and hyperboloid of two sheets (Fig. 1,c) [1, 2].

Hyperboloid surfaces are used in various fields, such as mathematics, physics, engineering, and architecture, due to their shape properties.

Hyperbolic surfaces can be found in the design of lenses and mirrors in optics, they can also be used to create objectives, and optical systems with specific properties, for example, control of the direction of light beams or aberration correction.

Additionally, the shape of hyperbolic surfaces can be used in directional antennas as they can efficiently focus and direct electromagnetic waves. Hyperboloids can be

a b c

Fig. 1. Hyperboloid: *a* – of one sheet; *b* – conical surface in between; *c* – two sheets.

[*] Corresponding author: P. I.Braileanu, Splaiul Independenței 313, București 060042, Romania.
Tel.: (+40) 21 402 94 11
E-mail addresses: patricia.braileanu@upb.ro (P. I. Braileanu)

used in the design of antennas (WIPL-D models [3]) for wireless communications and other signal transmission and reception applications but should not be confused with hyperbolic paraboloids.

They can also be found in architectural structures, where their surfaces are used to create unique and distinctive structures. For example, the Sagrada Familia Cathedral in Barcelona, designed by Antoni Gaudí, uses hyperbolic forms for towers and decorative elements [4], and the hyperbolic surfaces provide stability and an unmistakable aesthetic.

Hyperbolic surfaces are used in engineering for various applications, such as pressure pipes and tanks. Their resistant shape can withstand external pressures and loads, and they can be used in the construction of durable and cost-effective structures. These are just a few examples of the uses of hyperbolic surfaces. Due to their special mathematical and geometric properties, hyperboloids find applications in a wide range of fields.

This study considers the shape of a hyperboloid of one sheet to generate ten reinforced structures that can be used as supporting elements in industrial design products.

In mathematics, the hyperboloid of one sheet can be easily described by the following equation [1]:

$$\frac{x^2}{a^2}+\frac{y^2}{b^2}-\frac{z^2}{c^2}=1. \qquad (1)$$

where *a*, *b*, and *c* represent constants that determine the shape and scale of the hyperboloid, and *x*, *y*, and *z* are variables representing the coordinates of points on its surface. Equation (1) represents a three-dimensional surface with a single connected sheet that curves away from the axis of rotation.

Some examples of solid forms based on hyperboloids are as follows: stupa (a traditional Buddhist architectural form consisting of a dome-shaped structure that can be also obtained by rotating a hyperboloid of one sheet around its vertical axis) [5]; hyperbolic obelisks (three-dimensional solid forms obtained by rotating a hyperbola around its axis, which can be used as decorative elements in architecture or sculpture, characterized by an elongated and curved shape); abstract sculptures (hyperboloids can serve as a basis for three-dimensional abstract sculptures by modeling and combining multiple hyperboloids we can create interesting and innovative forms in the art of sculpture at various execution scales); structures within industrial design elements; structures within objects.

2. METHODS

A based structure design was chosen to be built starting from the geometry of a hyperboloid of one sheet, defining a small scale of this basic structure as indicated in Fig. 2,*a*. Subsequently, based on this model, 10 reinforced structures were built with ribs that follow the geometric curves of the initial shape, having a width of approximately 10 mm, a length of approximately 15 mm, and a height corresponding to the height's base structure (Fig. 2,*b*).

A total of 10 structures was designed using Inventor Professional 2023. These structures were subsequently analyzed, with the only differing element being the number of reinforcing ribs added to the basic three-dimensional geometry. The purpose of this analysis was to examine the effects of varying the number of ribs on the structural properties and performance of each geometry.

Table 1 provides a detailed overview of the differences between the various geometries. It highlights the specific characteristics and parameters associated with each structure, including the number of reinforcing ribs and other relevant factors considered in this study. By comparing the data presented in Table 1, we can gain insights into how each geometry mechanically behaves and understand the implications of the varying number of reinforcing ribs on the overall structural behavior.

Through this static study analysis, valuable information can be obtained regarding the influence of the number of reinforcing ribs on the stability, strength or other mechanical properties of these hyperboloid structures. This comprehensive examination allows for a better understanding of the relationship between the geometric design choices and the resulting structural performance, contributing to the development of optimized and efficient designs.

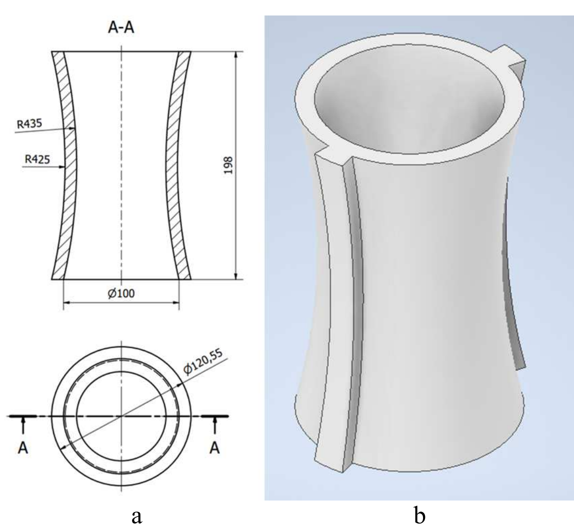

Fig. 2. Structure design: *a* – technical drawing; *b* – example of one of the reinforced structures.

Table 1

Number of reinforcement elements of the geometric structures used in this study

Geometric structure	No. of elements
H1	none
H2	2
H3	3
H4	4
H5	5
H6	6
H7	7
H8	8
H9	9
H10	10

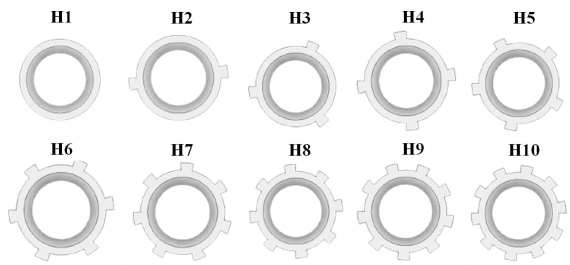

Fig. 3. Top view of the structures analyzed in this study.

It should be mentioned that as the number of reinforcing elements was increased, they were evenly distributed at equal distances between them as shown in Fig. 3.

2.1. Static study boundary conditions

Static study boundary conditions refer to the constraints and forces applied to a structure or system during a static analysis [7]. These boundary conditions define the external conditions and constraints that affect the behavior and response of the structure under applied loads.

Thus, it was necessary to fix the structure as indicated in Fig. 4.a. These boundary conditions restrict the movement of certain points or edges of the structure. They prevent translation and rotation in specific directions, providing stability.

Then a force of 1000 N was applied distributed on the upper face of the geometric structure as indicated in Fig. 4,*b*. Distributed loads, also known as uniformly distributed loads or surface loads, are applied forces or pressures that are spread over an area or along a line of a structure.

These boundary conditions were applied consistently in all variations of the structures with reinforcing elements in order to compare the obtained results.

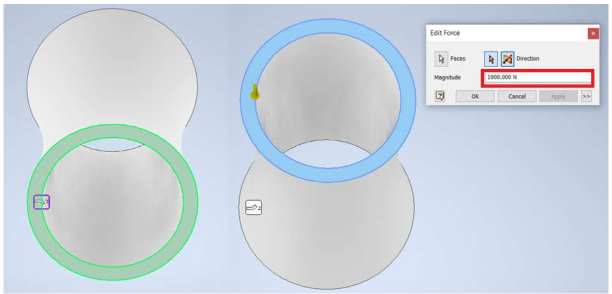

a b

Fig. 4. Static study boundary condition: *a* – structure fixture; *b* – force applied.

Table 2

General properties of ABS material

Mechanical properties	ABS
Behavior	Isotropic
Young's Modulus	2.24 GPa
Poisson's Ratio	0.38 ul
Density	1.06 g/cm^3
Yield Strength	20 MPa
Ultimate Tensile Strength	29.6 MPa
Shear Modulus	0.811594 GPa

2.2. Material applied

In this study, one thermoplastic material type was used on each individual geometry to observe the mechanical behavior of these structures under the applied load. The ABS (Acrylonitrile Butadiene Styrene) is a thermoplastic polymer widely used in industrial manufacturing [6]. This material was chosen for this case study because is commonly used in additive manufacturing, making it readily available for example in structures that can be 3D printed and assembled. The general properties of the material are shown in Table 2. The material settings used were taken from the material library of Autodesk Inventor Professional 2023.

Regarding the mesh details, the following settings were used for all the studied structures: an average element size (fraction of model diameter) of 0.1; a minimum element size (fraction of average size) of 0.2; a grading factor of 1.5; a maximum turn angle of 60 °; curved mesh elements were created.

3. RESULTS

In case of the base geometry (H1), the first one analyzed, the Von Mises stress recorded a maximum value of 0.5805 MPa and a minimum value of 0.1135 MPa. The displacement ranged from a minimum value of 0 mm to a maximum value of 0.03618 mm. As for the Equivalent Strain, the minimum value was $5.688 \cdot 10^{-5}$ and the maximum value was $2.385 \cdot 10^{-4}$. The results for H1 geometry are shown in Fig. 5.

The geometry reinforced with 2 ribs (H2) showed for the Von Mises stress recorded a maximum value of 0.5475 MPa and a minimum value of 0.0948 MPa. The displacement ranged from a minimum value of 0 mm to a maximum value of 0.03665 mm. As for the Equivalent Strain, the minimum value was $4.753 \cdot 10^{-5}$ and the maximum value was $2.249 \cdot 10^{-4}$. The results for H2 geometry are shown in Fig. 6.

The geometry reinforced with 3 ribs (H3) showed for the Von Mises stress recorded a maximum value of 0.5226 MPa and a minimum value of 0.1012 MPa. The displacement ranged from a minimum value of 0 mm to a maximum value of 0.03339 mm. As for the Equivalent Strain, the minimum value was $5.055 \cdot 10^{-5}$ and the maximum value was $2.146 \cdot 10^{-4}$. The results for H3 geometry are shown in Fig. 7.

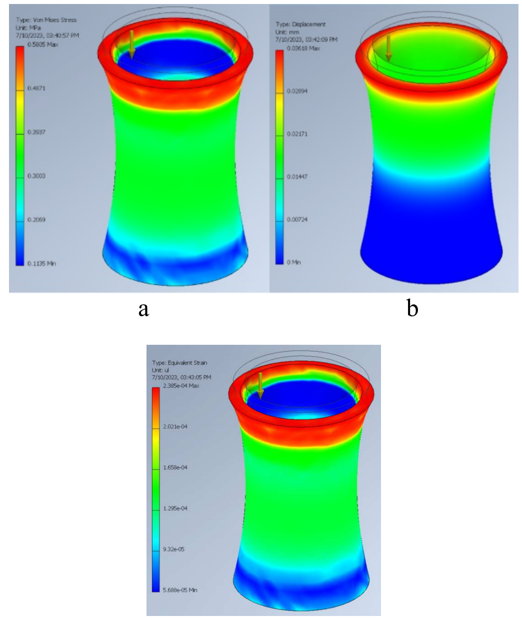

Fig. 5. H1 geometry static study results: *a* – Von Mises stress results; *b* – Displacement results; *c* – Equivalent Strain results.

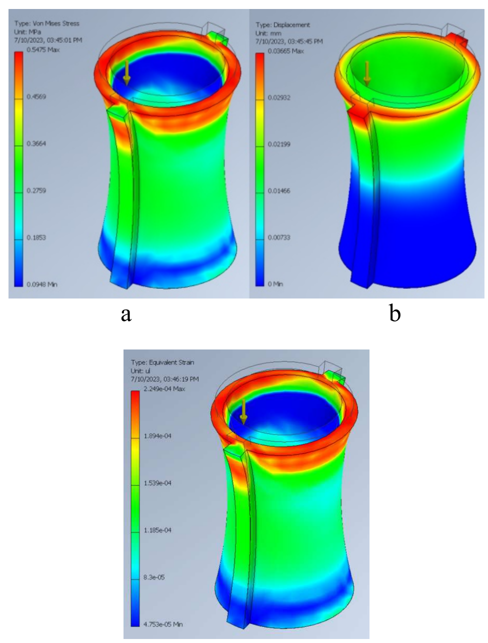

Fig. 6. H2 geometry static study results: *a* – Von Mises stress results; *b* – Displacement results; *c* – Equivalent Strain results.

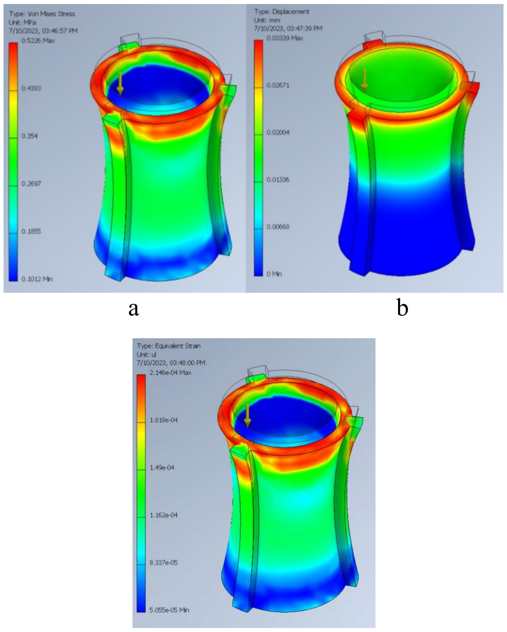

Fig. 7. H3 geometry static study results: *a* – Von Mises stress results; *b* – Displacement results; *c* – Equivalent Strain results.

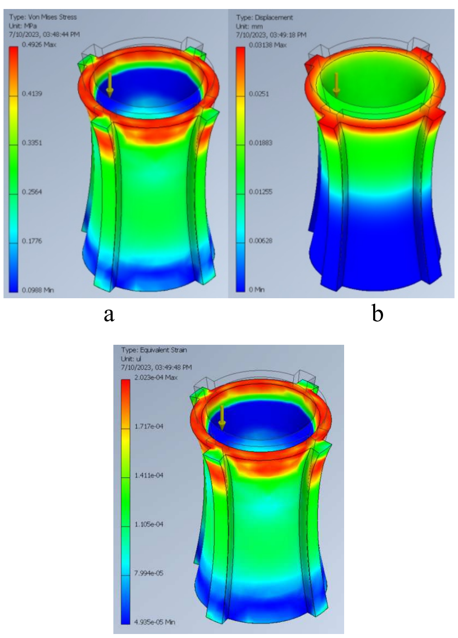

Fig. 8. H4 geometry static study results: *a* – Von Mises stress results; *b* – Displacement results; *c* – Equivalent Strain results.

The structure reinforced with 4 ribs (H4) showed for the Von Mises stress recorded a maximum value of 0.4926 MPa and a minimum value of 0.0988 MPa. The displacement ranged from a minimum value of 0 mm to a maximum value of 0.03138 mm. As for the Equivalent Strain, the minimum value was $4.935 \cdot 10^{-5}$ and the maximum value was $2.023 \cdot 10^{-4}$. The results for H4 geometry are shown in Fig. 8.

The 3D geometry reinforced with 5 ribs (H5) showed for the Von Mises stress recorded a maximum value of 0.4815 MPa and a minimum value of 0.0915 MPa. The

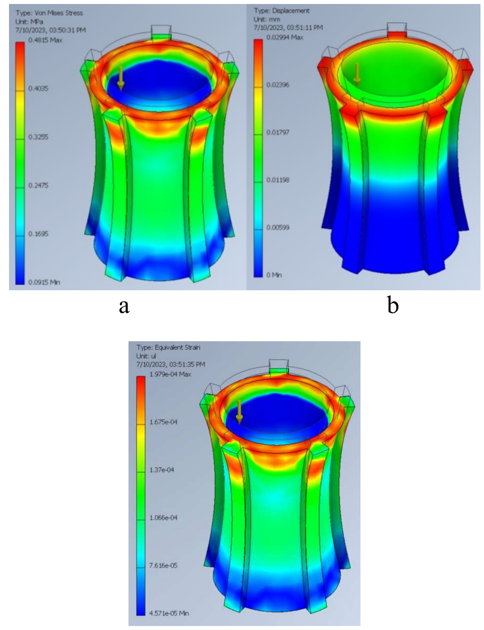

Fig. 9. H5 geometry static study results: *a* – Von Mises stress results; *b* – Displacement results; *c* – Equivalent Strain results.

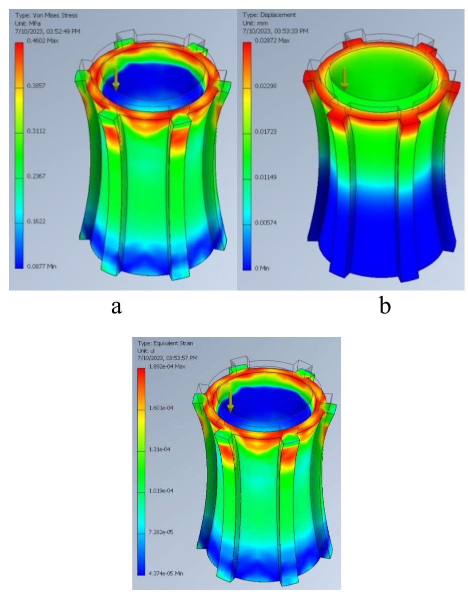

Fig. 10. H6 geometry static study results: *a* – Von Mises stress results; *b* – Displacement results; *c* – Equivalent Strain results.

displacement ranged from a minimum value of 0 mm to a maximum value of 0.02994 mm. As for the Equivalent Strain, the minimum value was $4.571 \cdot 10^{-5}$ and the maximum value was $1.979 \cdot 10^{-4}$. The results for H5 geometry are shown in Fig. 9.

The geometry reinforced with 6 ribs (H6) showed for the Von Mises stress recorded a maximum value of 0.4602 MPa and a minimum value of 0.0877 MPa. The displacement ranged from a minimum value of 0 mm to a maximum value of 0.02872 mm. As for the Equivalent Strain, the minimum value was $4.374 \cdot 10^{-5}$ and the maximum value was $1.892 \cdot 10^{-4}$. The results for H6 geometry are shown in Fig. 10.

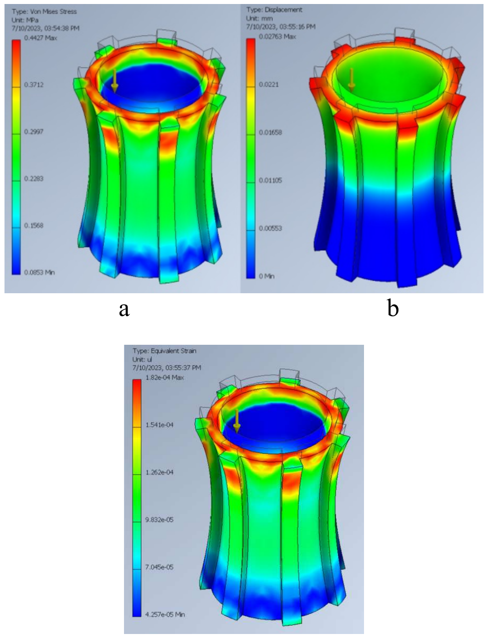

a b

c

Fig. 11. H7 geometry static study results: *a* – Von Mises stress results; *b* – Displacement results; *c* – Equivalent Strain results.

The structure reinforced with 7 ribs (H7) showed for the Von Mises stress recorded a maximum value of 0.4427 MPa and a minimum value of 0.0853 MPa. The displacement ranged from a minimum value of 0 mm to a maximum value of 0.02763 mm. As for the Equivalent Strain, the minimum value was $4.257 \cdot 10^{-5}$ and the maximum value was $1.82 \cdot 10^{-4}$. The results for H7 geometry are shown in Fig. 11.

The 3D geometry reinforced with 8 ribs (H8) showed for the Von Mises stress recorded a maximum value of 0.4242 MPa and a minimum value of 0.0825 MPa. The displacement ranged from a minimum value of 0 mm to a maximum value of 0.02661 mm. As for the Equivalent Strain, the minimum value was $4.067 \cdot 10^{-5}$ and the maximum value was $1.743 \cdot 10^{-4}$. The results for H8 geometry are shown in Fig. 12.

The 3D structure reinforced with 9 ribs (H9) showed for the Von Mises stress recorded a maximum value of 0.4055 MPa and a minimum value of 0.0785 MPa. The displacement ranged from a minimum value of 0 mm to a maximum value of 0.02567 mm. As for the Equivalent Strain, the minimum value was $3.913 \cdot 10^{-5}$ and the maximum value was $1.666 \cdot 10^{-4}$. The results for H9 geometry are shown in Fig. 13.

Finally, the geometry reinforced with 10 ribs (H10) showed for the Von Mises stress recorded a maximum value of 0.3968 MPa and a minimum value of 0.0808 MPa. The displacement ranged from a minimum value of 0 mm to a maximum value of 0.02482 mm. As for the Equivalent Strain, the minimum value was $4.024 \cdot 10^{-5}$ and the maximum value was $1.63 \cdot 10^{-4}$. The results for H10 geometry are shown in Fig. 14.

These results provide valuable knowledge into the structural behavior of the hyperboloid–based geometries and can be used to evaluate their performance under different loading conditions and rib configurations, depending on the structure applications.

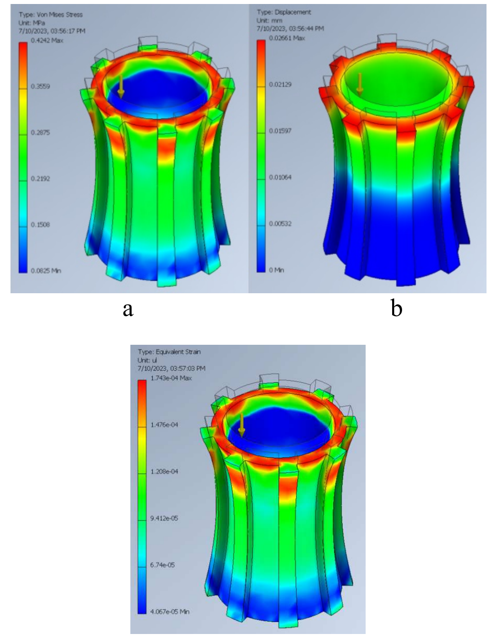

a b

c

Fig. 12. H8 geometry static study results: *a* – Von Mises stress results; *b* – Displacement results; *c* – Equivalent Strain results.

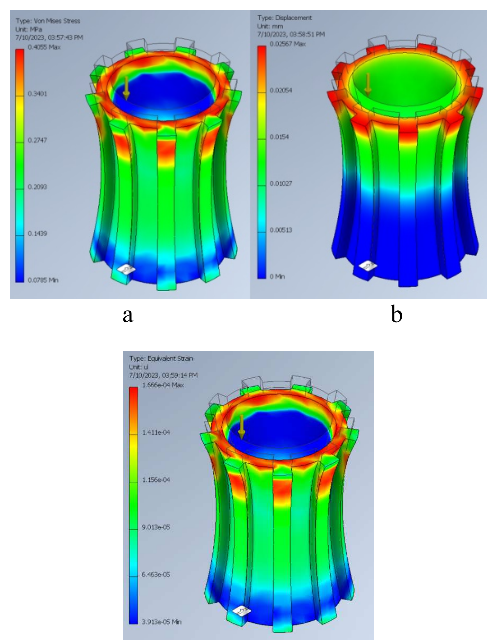

a b

c

Fig. 13. H9 geometry static study results: *a* – Von Mises stress results; *b* – Displacement results; *c* – Equivalent Strain results.

4. CONCLUSIONS

Hyperboloid–based structures, generated by rotating hyperbolic curves around an axis, have captured the attention of various fields due to their unique geometries and properties. This study aimed to analyze hyperboloid structures with reinforcing ribs, investigating their mechanical behavior and potential applications in different industries.

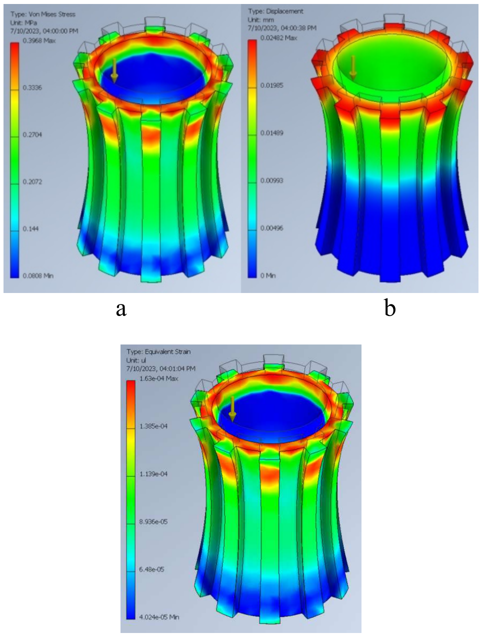

a b

c

Fig. 14. H10 geometry static study results: *a* – Von Mises stress results; *b* – Displacement results; *c* – Equivalent Strain results.

The results of the analysis revealed important insights into the mechanical performance of the structures. As the number of reinforcing ribs increased, significant improvements were observed, indicating enhanced structural stability and load-bearing capabilities.

One of the key findings was related to Von Mises stress, which decreased with the addition of reinforcing ribs. This suggested that the ribs effectively distributed the applied loads, minimizing stress concentrations and improving the overall integrity of the structures. By reducing stress, the hyperboloid–based structures with reinforcing ribs demonstrated increased resistance to deformation and failure.

In terms of displacement, the study showed that the addition of reinforcing ribs led to a reduction in the movement and deformation of the structures under load. This indicated that the ribs enhanced the rigidity and stability of the hyperboloid structures, making them suitable for applications where structural integrity is crucial.

Furthermore, the strain values exhibited a decreasing slope with the incorporation of reinforcing ribs, indicating that the ribs played a crucial role in reducing material deformation and ensuring the structures could withstand applied loads without exceeding their elastic limits. The improved strain characteristics demonstrated the potential of hyperboloid–based structures with reinforcing ribs for various industries, where structural stability is essential.

The practical implications of this study are far-reaching. In industrial design, hyperboloid structures with reinforcing ribs offer unique and efficient solutions for supporting elements, providing stability and load-bearing capabilities. In the field of architecture, these structures present visually striking aesthetics and can be used to create iconic architectural elements that combine stability with artistic expression.

In conclusion, the analysis of hyperboloid–based structures with reinforcing ribs demonstrated their enhanced mechanical performance and stability. The findings open doors to new possibilities in industrial design and architecture, where these structures can provide innovative solutions for supporting elements and create visually captivating designs. With further research and development, hyperboloid structures with reinforcing ribs have the potential to revolutionize various industries by offering efficient and aesthetically pleasing structural solutions.

REFERENCES

[1] Weisstein, Eric W., *One-sheeted hyperboloid*, available at: `https://mathworld.wolfram.com/One-SheetedHyperboloid.html`, accessed: 2023-06-02.

[2] Weisstein, Eric W., *Two-sheeted hyperboloid*, available at: `https://mathworld.wolfram.com/Two-SheetedHyperboloid.html`, accessed: 2023-06-02.

[3] WIPL-D Models, *Hyperboloid Lens Antenna Design Guide*, available at: www.wipl-d.com, accessed: 2023-05-14.

[4] Jin-Ho Park, *Early Shape Morphing: the Metamorphosis of Polygons in Antoni Gaudi's Sagrada Familia Cathedral and Le Corbusier's Firminy Shapel*, Journal of Asian Architecture and Nuilding Engineering, Vol.4, No. 1, May 2005, pp. 25–30.

[5] C. E. Porto, *A Comparative Architectural Study of the Structural Form between Two Religious Buildings in Brasília: The Cathedral and the Tibetan Stupa*, Journal of Civil Engineering and Architecture, Vol.7, No. 9, Sep. 2013, pp. 1092–1110.

[6] K. Gong, H. Liu, C. Huang, Z. Cao, E. Fuenmayor, I. Major, *A Comparative Hybrid Manufacturing of Acrylonitrile Butadiene Styrene (ABS) via the Combination of Material Extrusion Additive Manufacturing and Injection Molding*, Polymers, Vol.14, No. 23, Nov. 2022, 5093.

[7] N. S. Krivoshapko, *Static, vibration, and buckling analyses and applications to one-sheet hyperboloidal shells of revolution*, Appl. Mech. Rev, Vol.55, No. 3, 2002, pp. 241–270.